Thickening Mechanisms of Polyisobutylene in Polyalphaolefin

Michelle Len[†]
mlen2@ucmerced.edu

Uma Shantini Ramasamy[†]
uramasamy@ucmerced.edu

Seth Lichter[§]
s-lichter@northwestern.edu

✉ Ashlie Martini[†]
amartini@ucmerced.edu

[†]Department of Mechanical Engineering, University of California Merced, Merced, CA, USA
[§]Department of Mechanical Engineering, Northwestern University, Evanston, IL, USA

Received: 29 August 2017 / Accepted: 19 November 2017 / Published Online: 25 November 2017

Abstract

Molecular dynamics simulations are used to study the effect of polyisobutylene polymer on the viscosity of polyalphaolefin base oil. The Newtonian viscosities of the solution calculated from simulations at 40°C and 100°C agree with rheometer measurements. The simulations are used to investigate three possible mechanisms by which the polymer may increase solution viscosity. The results indicate that neither (i) coil expansion nor (ii) polymer-polymer association underlie viscosity enhancement in the case studied here. Measurements of solvent reorientation close to the additive molecule suggest that (iii) modification of the solvent by the additive molecule contributes to viscosity enhancement.

Introduction

The viscosity of a lubricant decreases as temperature increases during operation, which can result in dry-contact friction, component wear, and mechanical failure. This issue is addressed in most lubricant formulations by the use of viscosity modifiers (VMs). VMs are polymeric additives that increase the viscosity of lubricants, either uniformly at all temperatures, as thickeners, or more at higher temperatures, as viscosity index improvers (VIIs).

Several mechanisms have been proposed to explain the functionality of VMs. Two of them, coil expansion and polymer association, posit that the viscosity modification is due to the direct action of the polymer additive; the third mechanism relies on the additive

altering the characteristics of the solvent. Coil expansion is a widely accepted theory [1–4] which was first proposed in 1958 [5]. This theory states that, at lower temperatures, a polymer remains in a coiled conformation, and at higher temperatures, the polymer expands, thereby increasing viscosity more at higher temperature. Secondly, polymer association, characterized by interactions between polymer additives, serves as another mechanism that may influence viscosity. Forms of association such as entanglement and cross-links have been studied [6–10]. Finally, fluctuations of the solvent molecule, as they stretch and retract, dissipate energy which contributes to viscosity. The extent of energy dissipation relies on the solvent being stretched by the velocity gradients in the flow, which is influenced by the angular distribution of the solvent with respect to the gradient of velocity. Alternatively or concurrently, the additive may be moving at a velocity different from the local velocity of the solvent. When this occurs, the relative velocity of the solvent flowing past the additive molecule will increase the dissipation leading to an increase in viscosity. Whether due to the solvent itself or the motion of the solvent relative to the additive molecule, the angular distribution of the solvent (in a way to be made precise below) close to the additive molecule may differ from the distribution far from the additive molecule [8, 11].

In this work, molecular dynamics simulations are used to investigate the mechanisms underlying the functionality of polyisobutylene (PIB) VMs. PIB is selected for this study because it is a commonly used additive in many applications and its narrow molecular weight distribution enables direct comparison between experiments and simulations. Viscosity is calculated from simulations run at 40°C and 100°C on systems containing only polyalphaolefin (PAO) base oil and solutions of PAO with 10 wt.% PIB. Simulation results are validated by comparison to experimental measurements and then the atomic-scale details available in the simulations are used to explore the various VM mechanisms described above: coil expansion is quantified as the radius of gyration of PIB; polymer association is determined based on the contact time between two PIB molecules; and the interaction of the additive and solvent is investigated using the angular distribution of the solvent molecules. These mechanisms are characterized and then correlated to

temperature-viscosity behavior to determine how PIB polymers contribute to solution viscosity.

Methods

PAO 2cSt ($C_{20}H_{42}$) and 1348.6 g/mol PIB ($C_{96}H_{194}$) molecules were created using Materials Studio software (Accelrys Inc.). To model bulk fluids, the molecules were placed in simulation boxes with periodic boundaries and a 1:1:2 aspect ratio. Three models were created: pure PAO, 1 PIB in PAO, and 2 PIB's in PAO, as shown in Figure 1. The simulation box sizes were 2.5 × 2.5 × 5.0 nm^3, 2.4 × 2.4 × 4.8 nm^3 and 3.1 × 3.1 × 6.2 nm^3, respectively. Both the 1 and 2 PIB models were at 10 wt.% polymer concentration. Simulation dynamics were implemented using the Large Atomic/Molecular Massively Parallel Simulation (LAMMPS) software [12]. The All Atom Optimized Potentials for Liquid Simulations Force Field for Long Hydrocarbons (L-OPLS-AA) was used [13, 14]. A van der Waals 1-4 scaling factor of 0.0 was implemented to avoid non-bond interactions between atoms connected by three covalent bonds. This has been shown to give accurate density predictions for molecules containing more than 16 carbon atoms with the OPLS-AA force field [15], and we apply it here for L-OPLS-AA. A long-range solver for electrostatic interactions was not used in this work. A simulation timestep of 1.0 fs and a Nosé-Hoover thermostat and barostat were used to regulate temperature and pressure with damping coefficients of 100 and 1000 fs, respectively [16, 17].

For each model, energy minimization was followed by equilibration using NVT (constant number of atoms, volume and temperature) at 1000 K for 0.5 ns. Next, the systems were equilibrated using NPT (constant number of atoms, pressure and temperature) at 1 atm for 2 ns at the target temperature (40°C and 100°C). NPT was then repeated until the density at the last timestep matched the average density of the system. Finally, the systems were equilibrated under NVT again at their target temperature for approximately 0.5 ns.

Viscosity simulations were implemented on all of the systems using the Reverse Non-Equilibrium Molecular Dynamics (RNEMD) simulation method [18–20]. The RNEMD

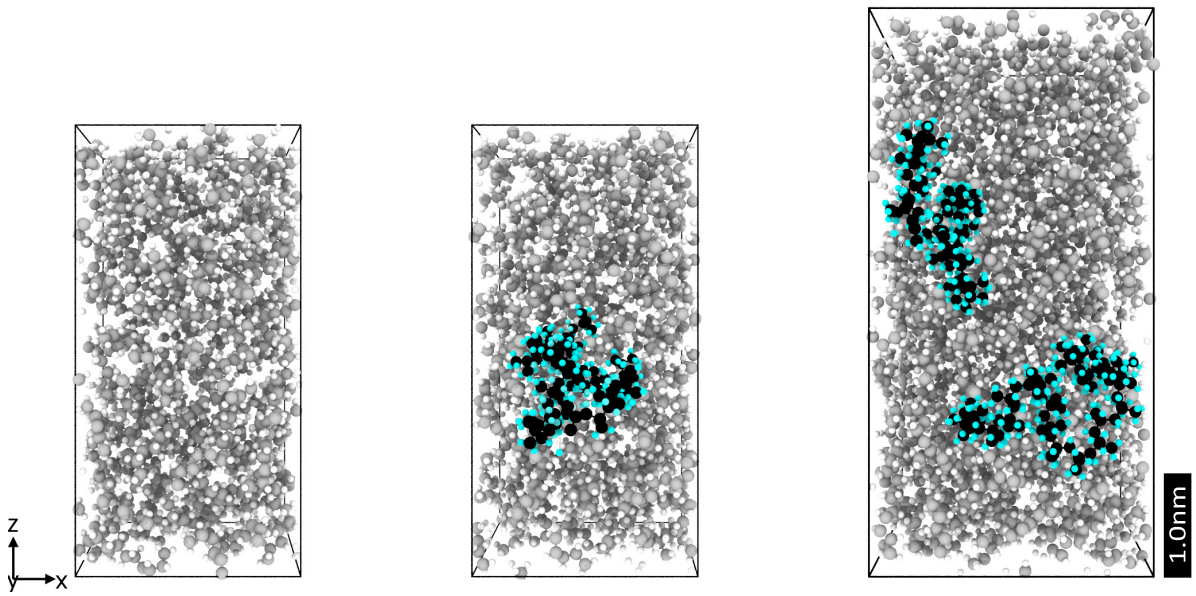

(a) (b) (c)

Figure 1: Initial configurations of (a) PAO base oil (b) one PIB molecule in PAO solvent and (c) two PIB molecules in PAO solvent, where the solid black lines indicate the periodic boundary. In PAO and PIB respectively, the white and blue spheres represent hydrogen atoms, and the gray and black spheres represent carbon atoms.

method divided the simulation box into twenty slabs or bins in the z-direction. A momentum flux was imposed on the system, creating a momentum exchange between the slabs such that the system underwent shear in the x-direction. The momentum flux and running time-averaged velocity profile data were output at each timestep. The average total flux (j_{xz}) was calculated after the flux reached steady-state. The shear rate was obtained from a linear fit to the average velocity profile data. The average shear rate ($\dot{\gamma}$) was calculated after the simulation reached steady-state. The viscosity (η) was then calculated from the average total flux and average shear rate using Equation 1:

$$\eta\left(\dot{\gamma}\right) = -\frac{j_{xz}}{\dot{\gamma}} \tag{1}$$

RNEMD equilibration was run for 4 ns before the production run. The slowest shear rate was used to determine the maximum run time required to reach steady-state, which was 100 ns. Subsequent simulations at faster shear rates had production runs between 50 and 100 ns. Only viscosities obtained from simulations where the goodness of the linear

fit to the average velocity profile was $R^2 > 98.5\%$ were used in subsequent analyses. The shear viscosity data for each system was fit to the Carreau model, Equation 2:

$$\eta\left(\dot{\gamma}\right) = \frac{\eta_0}{[1 + (\lambda\dot{\gamma})^2]^p} \tag{2}$$

where η_0 is the viscosity at zero shear rate (Newtonian viscosity), λ is the relaxation time constant, and p is the strain rate sensitivity coefficient [20]. Although the simulations could only capture viscosities at high shear rates, the Newtonian viscosity was extrapolated using the Carreau model [21].

The radius of gyration, R_g, of the PIB polymers was calculated after the relaxation and equilibration processes from NVT simulations run for 100 ns at 40°C and 100°C under non-shear conditions. This calculation was performed without shear because it assumes a spherical shape, which may not be the case when the polymer is being sheared. Also, the approach is consistent with direct experimental measurements of polymer R_g [22, 23], which are necessarily under non-shear conditions. R_g is calculated from the distance between atoms in the polymer and the polymer's center of mass using Equation 3:

$$R_g = \sqrt{\frac{1}{M}\sum_i m_i(\mathbf{r}_i - \mathbf{r}_{cm})^2} \tag{3}$$

where M is the total mass of the molecule, i is the atom index, m_i is the mass of atom i, $\mathbf{r}_i$ is the position of atom i, and $\mathbf{r}_{cm}$ is the center of mass position of the polymer. The R_g was calculated every 5 ps during a 20-ns NVT simulation and plotted as frequency histograms, consistent with a previous approach [21, 22, 24].

Association between two PIBs was quantified using an algorithm that calculated the minimum distance between each carbon atom in one polymer and the carbon atoms in the other polymer. The atoms whose minimum distance was within a specified cutoff radius were considered to be in "contact" based on the concept of atomic contact used for nanoscale junctions between solids [25]. The cutoff radius was selected as 0.59 nm, which is approximately twice the distance at the minimum of the Lennard-Jones energy between two carbon atoms. The cutoff is arbitrary, so the number of contact atoms itself

is not meaningful. However, a larger number of contact atoms is assumed to correspond to more association between the two polymers, so the value can be used to compare from case to case.

Simulation predictions of viscosity were compared to experimental viscosity measurements of 10 wt.% PIB in 2 cSt PAO. The measurements were obtained using a Cannon StressTech HR Oscillatory Rheometer. Indopol H-300 with a molecular weight of approximately 1300 g/mol obtained from Ineos was used as the PIB sample due to its comparable molecular weight to the simulated model. A PAO 2cSt base stock obtained from Chevron Phillips was used as the solvent. The PIB sample was blended into the PAO in a beaker on a hot plate at 70°C at 500 rpm until the solution was completely dissolved, where the solution was homogeneous and no PIB clumps were visibly present on the bottom of the beaker. A bob and cup setup and constant shear rate (100 s^{-1}) method on the rheometer were used to measure Newtonian viscosity.

Results and Discussion

Viscosities as a function of shear rate calculated from simulations of pure PAO, PAO with 10 wt.% PIB modeled with 1 PIB molecule and PAO with 10 wt.% PIB modeled with 2 PIB molecules, at 40 and 100°C, are shown in Figure 2. The data points are fit to the Carreau equation (dashed lines in Figure 2) to enable extrapolation to the Newtonian viscosities. For the pure PAO system, the Newtonian viscosities are 3.59 ± 0.07 cP and 1.12 ± 0.02 cP at 40°C and 100°C, respectively. These values are slightly below what is expected for a 2 cSt at those two temperatures, i.e. 3.98 and 1.28 cP, indicating the simulations may under-predict viscosities in this range. However, it is important to note that this represents a relatively small viscosity under-prediction in MD simulations of long chain molecules (10.3% at 40°C and 11.7% at 100°C), which is consistent with previous observations for other hydrocarbons [26, 27] and demonstrates the efficacy of the L-OPLS-AA force-field used for PAO.

For the PIB systems, we observe that the difference between the viscosities of the models with 1 PIB and 2 PIB is statistically insignificant, so both sets of data points are

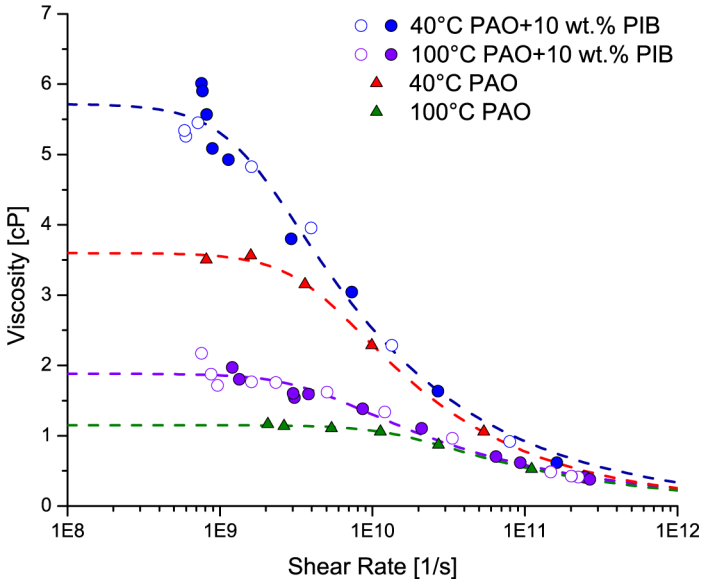

Figure 2: Viscosity calculated from simulations of pure PAO (triangles) and 10 wt.% PIB in PAO (circles) over a range of shear rates at 40°C and 100°C. Solid circles correspond to the 1 PIB model, and open circles correspond to the 2 PIB model. The dashed lines indicate the Carreau fits to each set of data, where the 1 PIB and 2 PIB data sets are combined at their respective temperatures.

used in the Carreau fits to increase the confidence in the resultant extrapolated Newtonian viscosities. The Newtonian viscosities of the PIB system are 5.72 ± 0.17 cP and 1.88 ± 0.04 cP at 40°C and 100°C, respectively. These results are compared to measurements from a benchtop rheometer, as illustrated in Figure 3. The differences between the mean experiment and simulation viscosities are 0.09 cP (1.5%) at 40°C and 0.43 cP (29.6%) at 100°C. However, at both temperatures, the results are in agreement within the statistical uncertainty of the measurements and calculations. Note that the large error bar for the simulation data at 40°C is due to the lack of data near the Newtonian plateau which results in uncertainty in the Newtonian viscosity obtained from the Carreau fit, and the large error bar in the experimental data at 100°C reflects the fact that this viscosity is near the lower limit of the rheometer's measurement capability.

A VM can be characterized as either a VII or a thickener, where the former increases a solution's viscosity more at high temperatures than at low temperatures, whereas the latter uniformly increases viscosity at all temperatures [28]. The distinction between a VII and a thickener can be made using a metric known as the Q factor, which is defined

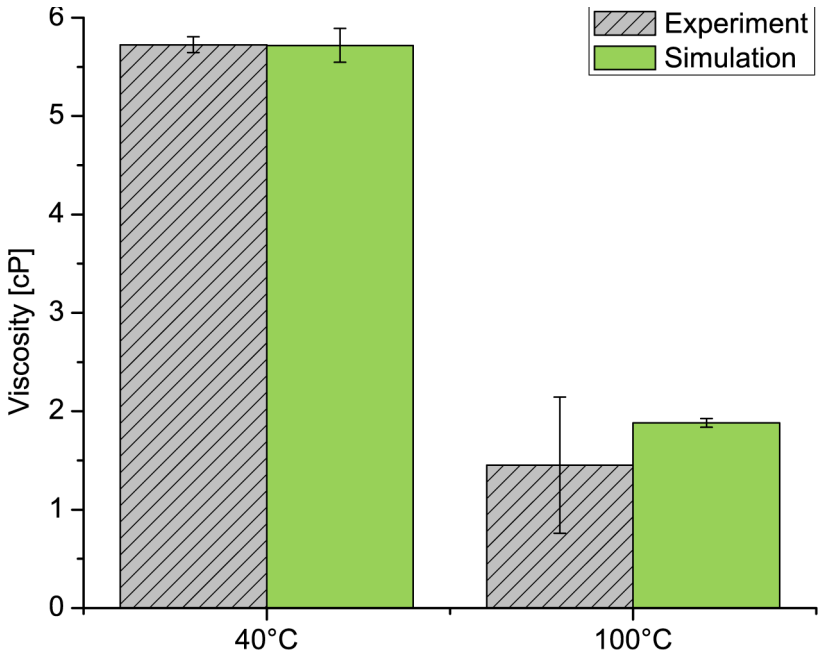

Figure 3: Comparison of the Newtonian viscosity of PAO with 10 wt.% PIB from simulations and experiments. The error bars for the experimental data reflect the accuracy of the rheometer based on measurements of standard fluids with comparable viscosity to the PAO/PIB solutions at each temperature. Error bars on the simulation viscosities represent the uncertainty associated with fitting the Carreau equation to the simulation data.

as:

$$Q = \frac{\eta_{sp}(100°\mathrm{C})}{\eta_{sp}(40°\mathrm{C})} \tag{4}$$

$$\eta_{sp} = \frac{\eta_{\mathrm{solution}} - \eta_{\mathrm{solvent}}}{\eta_{\mathrm{solvent}}} \tag{5}$$

where η_{sp} is the specific viscosity, η_{solution} is the viscosity of the polymer-enhanced solution, and η_{solvent} is the viscosity of the solvent. A value of $0 < Q < 1$ indicates that the molecule has less thickening power at high temperature, characteristic of a thickener, and a value of $Q > 1$ indicates that the molecule has more thickening power at high temperatures, characteristic of a VII [28, 29]. Simulation viscosities obtained for PIB at 40°C and 100°C are used to calculate a Q factor of 1.1, which indicates that the PIB polymer is a weak viscosity index improver. Note that we are unable to validate the simulation-calculated Q factor directly due to the large uncertainty in the experimental data at 100°C which leads to a wide range of Q factors that spans from less than 1 to above 1.

As mentioned previously, coil expansion, polymer association and additive/solvent

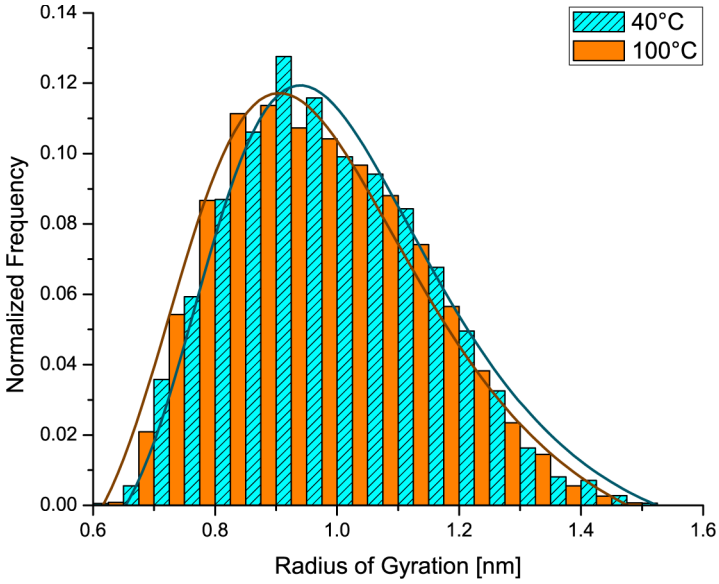

Figure 4: Histograms of the radius of gyration of the PIB systems at 40°C and 100°C where the solid lines are asymmetrical skew fits to the histograms.

interaction have been proposed to quantify how polymers increase viscosity. The possible contribution of each of these mechanisms to the solution viscosity is tested using the atomic-scale details available in the simulations.

First we characterize coil expansion, which is quantified by the radius of gyration, R_g, of the polymer [22, 23, 30–32]. We observe no statistically significant difference between the results from the 1 PIB and the 2 PIB systems, so the R_g values of the 1 and 2 PIB systems are combined into a single histogram at each temperature. An asymmetrical skew function is fit to the histogram data to obtain the mean R_g of the distribution. Figure 4 shows the frequency distributions and asymmetrical skew curve fits of the PIB's R_g at 40°C and 100°C. The mean R_g calculated from the skew curve fit is 0.94 nm at 40°C and 0.91 nm at 100°C, which suggests that the PIB does not expand with temperature. Therefore, the coil expansion mechanism is not observed. This is consistent with observations that have been made for other VMs, including olefin copolymers, in both experiments [22, 23, 33] and simulations [24].

The second mechanism studied is polymer association. In this work, polymer association is defined as two PIB polymers coming together in close proximity, which is quantified as the time over which contact pairs are present between the two polymers, where more contact-pair time is assumed to correspond to more association. The concept

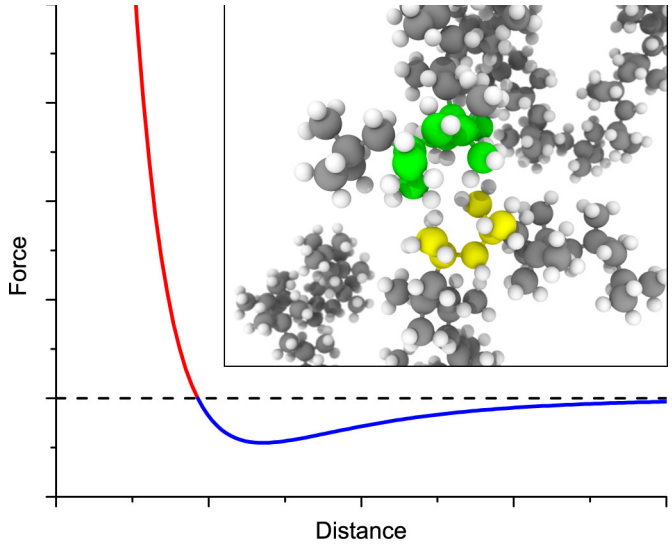

Figure 5: Plot of the Lennard-Jones interaction force vs. distance between two carbon atoms. The red curve corresponds to repulsive forces and the blue curve correspond to attractive interactions. In the fictitious "repulsive" system, the two PIBs only experience repulsive interaction from one another. The inset shows a zoomed-in image of two PIBs where the carbon atoms in "contact" are highlighted in yellow and green. Non-contact carbon atoms are represented in gray and hydrogen atoms are represented in white.

of contact pairs is illustrated in the inset to Figure 5(b), where the green and yellow atoms are in contact.

To determine if association increases viscosity for this system, a fictitious model is created where the interaction forces between the two PIB molecules are modified to be only repulsive. As illustrated in Figure 5, the non-bonded Lennard-Jones interaction contains repulsive (red) and attractive (blue) contributions: this is referred to as the "attractive" system. In the fictitious model, the only interactions between atoms in the two polymers is repulsive and this system is referred to as the "repulsive" system. The number of contact atoms for attractive and repulsive systems at both temperatures is calculated from simulations at shear rates of $\sim 1.4 \times 10^9$/s (the shear rate is approximate because the same imposed flux in RNEMD gives slightly different shear rates from case to case). Figure 6(a) shows the percent of the simulation time during which the two polymers are in contact, i.e. one or more pairs of atoms are in contact as defined above. At both temperatures, the polymers spend much less time in contact in the repulsive model than in the attractive model. This indicates that the modification of the interaction energy effectively decreases polymer-polymer association.

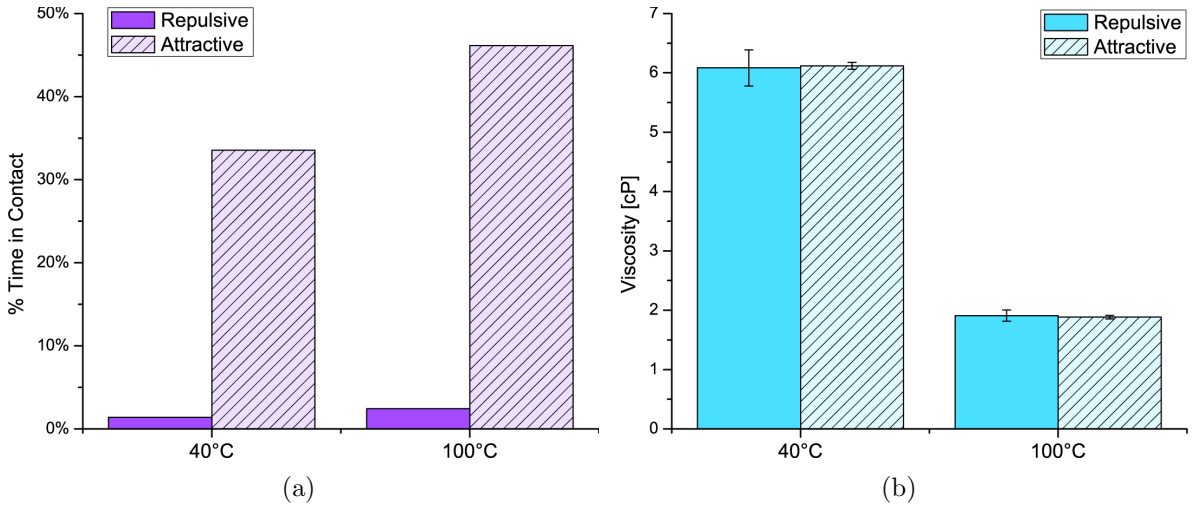

Figure 6: (a) Percent of simulation time during which the contact between two polymers is comprised of at least one pair of "contact" atoms. (b) Simulation-calculated Newtonian viscosities for both attractive and repulsive systems at the same temperatures where error bars represent the uncertainty associated with fitting the Carreau equation to the simulation data. The change in contact time shown in (a) does not yield any significant change in viscosity, as shown in (b).

Viscosity simulations are run for the repulsive system and the Newtonian viscosity is extracted from the Carreau fit to the data, following the same process applied to the attractive system. Figure 6(b) shows the extracted Newtonian viscosities for both systems at 40°C and 100°C. The differences between the viscosities of the attractive and repulsive systems are statistically insignificant at both temperatures; correspondingly, the Q factors for the two systems are nearly identical. This implies that, even though the PIBs come into close proximity to one another more often in the attractive model, this does not result in an increase of viscosity. Therefore, these findings show that polymer association does not appear to be contributing significantly to the effect of PIB on solution viscosity in this model system. However, it should be noted that the relatively small size of the model and the fact that there are just two polymers means that longer range, group effects may not be captured. Therefore, these results cannot be extrapolated to suggest that association would not be a contributing factor for PIB in general.

Polymer additives can increase viscosity through the interaction between the additive and solvent. To investigate the effect of the additive on the solvent molecules, the alignment of the solvent PAO molecules with respect to the flow direction is characterized.

This is quantified as L_x, the projection of the end-to-end length of the PAO molecule along the shear direction (x-direction), calculated from simulations at approximately the same shear rate as in the association analysis. The branched PAO molecules are expected to be present in a variegated set of conformations where the PAO geometry at any instant in time would be described by a large number of degrees of freedom. We do not account for the variety of PAO conformations and recognize that L_x is not a true measure of angular orientation. However, subsuming all the conformational complexity into one number L_x, that we refer to as the "orientation" or "alignment", gives us a simple operational means to explore if there may be changes in PAO or its orientation relative to the flow due to the presence of PIB. With this simplification, increases in L_x are interpreted as increasing alignment with the flow: $L_x = 0$ nm indicates a PAO molecule transverse to the flow; $L_x = 2.1$ nm is a molecule aligned with the flow.

Next, the PAO molecules are grouped into "close" and "far" categories. PAO molecules are placed in the "close" group if they contain carbon atoms that are within 0.59 nm of any carbon atom in the PIB (same criterion as used to determine contact between PIB molecules). All other PAO molecules are placed in the "far" group. This concept is illustrated in Figure 7(a) where PAO molecules in the close group are highlighted in yellow; all other PAO molecules are in the far group. L_x is calculated for each group throughout the simulation and the data presented as frequency histograms, as shown in Figures 7(b) and 7(c). An asymmetrical skew function is fit to each histogram to obtain the mean value of L_x of the distribution. The difference between the mean L_x of the close and far groups is found to be negligible, i.e. less than 0.01 nm at both 40°C and 100°C. This indicates that the effect of the polymer on solvent alignment cannot be captured by the mean L_x.

However, closer inspection of Figures 7(b) and 7(c) reveals that the number of molecules with L_x less than the mean value in the close group is larger than the far group. To quantify this observation, the number of molecules to the left of the mean L_x was calculated to be 44.2% and 43.0% for the close and far distributions at 40°C, respectively, and 47.7% and 46.3% for the close and far distributions at 100°C. At both temperatures, there is a

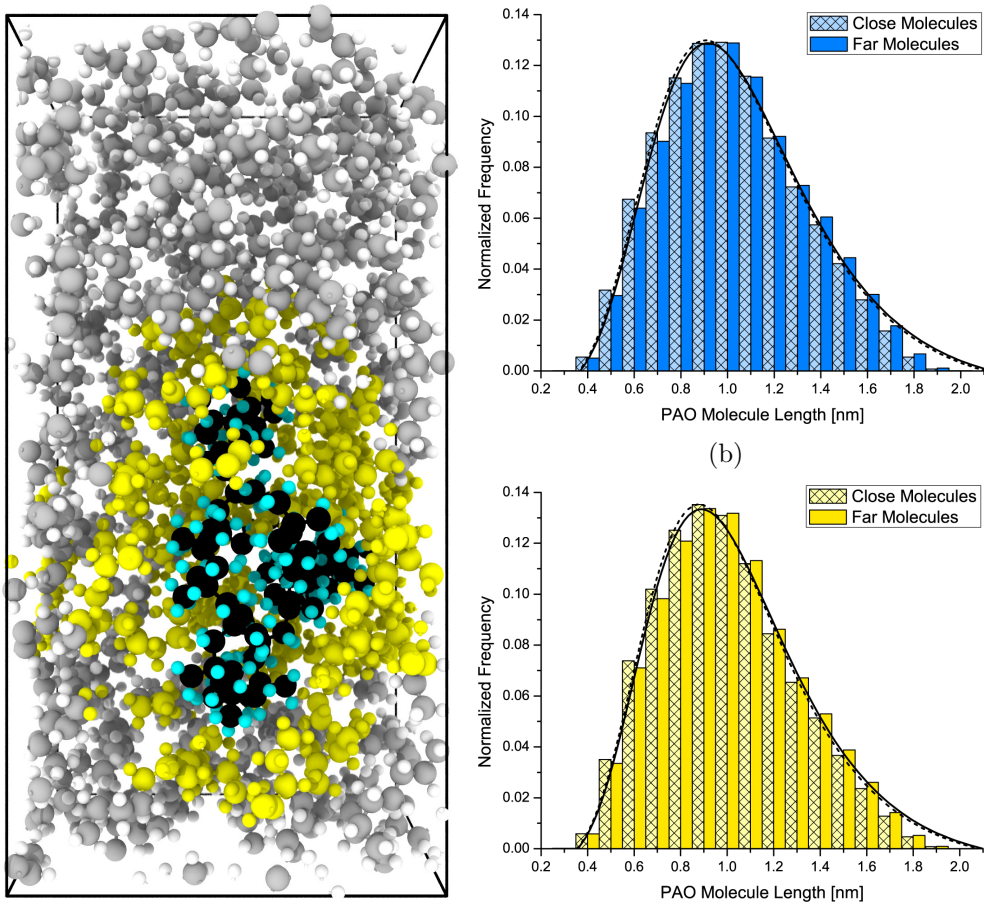

Figure 7: (a) Snapshot of a model system containing 1 PIB where the PAO atoms within 0.59 nm of the PIB are highlighted in yellow; PAO molecules containing these atoms are identified as "close". (b) Distribution of the close and far PAO molecule lengths of the system at 40°C. (c) Distribution of the close and far PAO molecule lengths of the system at 100°C. The dashed (solid) curve on the histogram is the asymmetrical skew distribution fit for the close (far) group of PAO molecules.

larger percentage of smaller values of L_x in the close group than the far group, indicating that there is evidence of change of orientation of PAO molecules near the PIB.

To highlight the difference between the fraction of close PAO molecules compared to the fraction of far PAO molecules, the value $\mathcal{R}(L_x)$ is defined:

$$\mathcal{R}(L_x) = \frac{N_{\text{close}}(L_x)}{\sum\limits_{L_x} N_{\text{close}}(L_x)} - \frac{N_{\text{far}}(L_x)}{\sum\limits_{L_x} N_{\text{far}}(L_x)}, \tag{6}$$

where $N_{\text{close}}(L_x)$ is the number of PAO molecules in the bin with length L_x that are assigned to the close group, the sum $\sum N_{\text{close}}(L_x)$ is the total number of PAO molecules

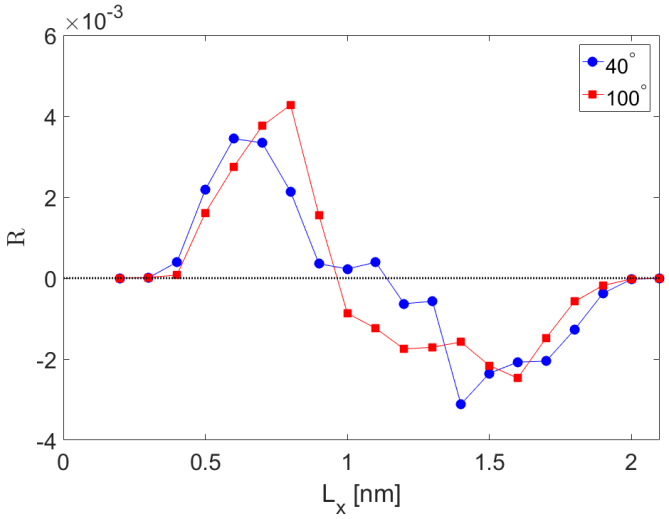

Figure 8: For a given orientation L_x, the difference $\mathcal{R}$ (see Equation 6) between the fraction of PAO molecules close to the PIB molecule minus the fraction far from the PAO molecule. The definitions of "close" and "far" are given in the text. The blue (red) data points are at 40° (100°). The positive values at smaller values of L_x indicate that PAO molecules located near PIB tend to be less aligned with the flow than those further from the PIB molecule.

in the close group, and similarly for the far molecules. $\mathcal{R} > 0$ indicates an orientation of PAO that tends to be close to the PIB; $\mathcal{R} < 0$ indicates an orientation of PAO that tends to be far from the PIB. The results of this calculation are shown in Figure 8. We observe that $\mathcal{R}$ is greater than zero for less-aligned PAOs and smaller than zero for more-aligned PAOs. This indicates that PAO molecules more aligned with the flow have a consistent tendency to be further from the PIB, while PAO molecules oriented more transverse to the flow have a consistent tendency to cluster near the PIB molecule. Note, too, that the sum of $\mathcal{R}$ over all lengths is equal to zero, that is, $\sum_{L_x} \mathcal{R} = 0$. While this normalization of Equation 6 enforces the condition that the likelihood of any length PAO to be close is equal to the likelihood of being far, the figure shows that PAO molecules less (more) aligned with the flow–and with correspondingly smaller (larger) values of L_x–are more likely to be found close to (far from) the PIB molecule.

Conclusions

In summary, molecular dynamics simulations were used to study the effect of PIB VMs on the viscosity of a PAO base oil. The ability of the simulations to accurately model this system was evidenced by reasonable agreement with experimentally-measured viscosities. The behavior of the viscosity as a function of temperature was characterized using the Q factor, which indicated that PIB is a weak VII in which the polymer increased the viscosity of the solution slightly more at higher temperatures. The mechanisms by which the PIB increased viscosity were then explored using the simulations. First, the role of coil expansion was characterized using the radius of gyration of the PIB molecule. No shift in the distribution towards larger radii of gyration with temperature was observed, which indicates that the coil size mechanism does not contribute to the effect of PIB on solution viscosity. Next, the effect of association between PIB molecules was quantified as the time that PIB molecules were in "contact". There was more polymer-polymer contact at 100°C than 40 °C, which may suggest that association is a contributing factor. This hypothesis was then tested by creating a fictitious model system in which the two PIB molecules interacted with each other only via repulsive forces. The new model successfully minimized the number of contact atoms, but did not affect the solution viscosity, which suggests that the association mechanism does not play a major role in PIB function as well, at least for the 2 PIB model here. Lastly, we studied the effect of the PIB on the alignment of the PAO using the length of the PAO in the shear direction as a simple approximation of molecular orientation of the solvent PAO molecules. A comparison of the lengths of the PAO molecules near and far from the PIB revealed less-aligned PAO molecules were more likely to be found closer to the PIB than further away. This result suggests that the PIB may be increasing viscosity indirectly through its effect on nearby PAO. Here we have shown that solvent alignment contributes to viscosity increase in a PIB/PAO system. This mechanism may be also relevant to other polymer/base oil combinations, but analyses similar to those demonstrated here should be performed with other model systems to determine how generally applicable the mechanism might be.

Acknowledgments

We thank David Gray, Joan Souchik and Paul Michael for useful discussion and feedback related to viscosity modifiers. We also acknowledge the Donors of the American Chemical Society Petroleum Research Fund (Grant #55026-ND6), National Science Foundation Engineering Research Center for Compact and Efficient Fluid Power EEC 05440834, and the National Fluid Power Association Education and Technology Foundations Pascal Society for support of this research.

References

[1] N. Canter. Viscosity index improvers. *Tribol. Lubr. Technol.*, 67(9), 2011.

[2] P. Ghosh and M. Das. Study of the influence of some polymeric additives as viscosity index improvers and pour point depressants synthesis and characterization. *J. Pet. Sci. Eng.*, 119:79–84, 2014.

[3] A. M. Nassar. Synthesis and evaluation of viscosity index improvers and pour point depressant for lube oil. *Pet. Sci. Technol.*, 26(8):523–531, 2008.

[4] T. Stöhr, B. Eisenberg, and M. Müller. A new generation of high performance viscosity modifiers based on comb polymers. *SAE Int. J. Fuels Lubr.*, 1(1):1511–1516, 2008.

[5] T. W. Selby. The non-newtonian characteristics of lubricating oils. *ASLE Trans.*, 1(1):68–81, 1958.

[6] P. G. de Gennes. Reptation of a polymer chain in the presence of fixed obstacles. *J. Chem. Phys.*, 55(2):572–579, 1971.

[7] J. D. Ferry. Viscoelastic properties of polymer solutions. *J. Res. Nat. Bur. Stand.*, 41(1):53–61, 1948.

[8] J. E. Glass, D. N. Schulz, and C. F. Zukoski. *Polymers as Rheology Modifiers*, chapter 1, pages 2–17. 1991.

[9] R. Longworth and H. Morawetz. Polymer association. IV. Hydrogen bonding and melt viscosities in copolymers of styrene with methacrylic acid. *Journal of Polymer Science*, 29(119):307–319, 1958.

[10] A. Yekta, B. Xu, J. Duhamel, H. Adiwidjaja, and M. A. Winnik. Fluorescence studies of associating polymers in water: Determination of the chain end aggregation number and a model for the association process. *Macromolecules*, 28(4):956–966, 1995.

[11] P. E. Rouse, Jr. A theory of the linear viscoelastic properties of dilute solutions of coiling polymers. *J. of Chem. Phys.*, 21(7):1272–1280, 1953.

[12] S. Plimpton. Fast parallel algorithms for short–range molecular dynamics. *J. Comput. Phys.*, 117(1):1–19, 1995.

[13] W.L. Jorgensen, D.S. Maxwell, and J. Tirado-Rives. Development and testing of the OPLS all-atom force field on conformational energetics and properties of organic liquids. *J. Am. Chem. Soc.*, 118(45):11225–11236, 1996.

[14] S. W. I. Siu, K. Pluhackova, and R. A. Böckmann. Optimization of the OPLS-AA force field for long hydrocarbons. *J. Chem. Theory Comput.*, 8(4):1459–1470, 2012.

[15] X. Ye, S. Cui, Valmor F. de Almeida, and B. Khomami. Effect of varying the 1-4 intramolecular scaling factor in atomistic simulations of long-chain n-alkanes with the opls-aa model. *J. Mol. Model.*, 19(3):1251–1258, 2013.

[16] Shūichi Nosé. A molecular dynamics method for simulations in the canonical ensemble. *Mol. Phys.*, 52(2):255–268, 1984.

[17] William G. Hoover. Canonical dynamics: Equilibrium phase-space distributions. *Phys. Rev. A*, 31:1695–1697, Mar 1985.

[18] M. S. Kelkar, J. L. Rafferty, E. J. Maginn, and J. I. Siepmann. Prediction of viscosities and vapor-liquid equilibria for five polyhydric alcohols by molecular simulation. *Fluid Phase Equilib.*, 260:218–231, 2007.

[19] F. Müller-Plathe. Reversing the perturbation in nonequilibrium molecular dynamics: An easy way to calculate the shear viscosity of fluids. *Phys. Rev. E*, 59:4894–4898, 1999.

[20] C. M. Tenney and E. J. Maginn. Limitations and recommendations for the calculation of shear viscosity using reverse nonequilibrium molecular dynamics. *J. Chem. Phys.*, 132(1):014103, 2010.

[21] U. S. Ramasamy, M. Len, and A. Martini. Correlating molecular structure to the behavior of linear styrene–butadiene viscosity modifiers. *Tribol. Lett.*, 65(4):147, 2017.

[22] P. Bhattacharya, U. S. Ramasamy, S. Krueger, J. W. Robinson, B. J. Tarasevich, A. Martini, and L. Cosimbescu. Trends in thermoresponsive behavior of lipophilic polymers. *Ind. Eng. Chem. Res.*, 55(51):12983–12990, 2016.

[23] M. J. Covitch and K. J. Trickett. How polymers behave as viscosity index improvers in lubricationg oils. *Adv. Chem. Engineer. Sci.*, 5(2):134–151, 2015.

[24] U. S. Ramasamy, S. Lichter, and A. Martini. Effect of molecular-scale features on the polymer coil size of model viscosity index improvers. *Tribol. Lett.*, 62(23):1–7, 2016.

[25] T.B.D. Jacobs and A. Martini. Measuring and understanding contact area at the nanoscale: A review. *Appl. Mech. Rev.*, 69:061101, 2017.

[26] W. Allen and R. L. Rowley. Predicting the viscosity of alkanes using nonequilibrium molecular dynamics: Evaluation of intermolecular potential models. *J. Chem. Phys.*, 106(24):10273–10281, 1997.

[27] J. P. Ewen, C. Gattinoni, F. M. Thakkar, N. Morgan, H. A. Spikes, and D. Dini. A comparison of classical force-fields for molecular dynamics simulations of lubricants. *Materials*, 9(8), 2016.

[28] P. Cusseau, N. Bouscharain, L. Martinie, D. Philippon, P. Vergne, and F. Briand. Rheological considerations on polymer-based engine lubricants: Viscosity index improvers versus thickeners - generalized newtonian models. *Tribol. T.*, 2017.

[29] H. Singh and I.B. Gulati. Influence of base oil refining on the performance of viscosity index improvers. *Wear*, 118(1):33–56, 1987.

[30] P. J. Flory. *Principles of Polymer Chemistry*. Cornell University Press, 1953.

[31] A. Y. Grosberg and D. V. Kuznetsov. Quantitative theory of the globule-to-coil transition. 1. link density distribution in a globule and its radius of gyration. *Macromolecules*, 25(7):1970–1979, 1992.

[32] J. Mazur and D. McIntyre. The determination of chain statistical parameters by light scattering measurements. *Macromolecules*, 8(4):464–476, 1975.

[33] C. Mary, D. Phillipon, L. Lafarge, D. Laurent, F. Rondelez, S. Bair, and P. Vergne. New insight into the relationship between molecular effects and the rheological behavior of polymer-thickened lubricants under high pressure. *Tribol. Lett.*, 52:357–369, 2013.